# Combined Tracking of the Maximum Power and Maximum Efficiency Operating Points for Real-Time Maximization of the Energy Production of PV Systems

Eftichios Koutroulis ⓘ, *Senior Member, IEEE*, Nektarios Sason, and Vasileios Georgiadis ⓘ

*Abstract*—The power production of a photovoltaic (PV) system can be maximized by applying a global maximum power point tracking (MPPT) method for ensuring that the PV array operates at the global MPP where its power production is maximized and, simultaneously, by dynamically maximizing the efficiency of the power converter that interfaces the PV-generated energy to the energy storage devices or the electric grid. In this paper, a new control method has been presented for the real-time maximization of the power production of PV systems by modifying in real time the duty cycle and switching frequency of the power converter PWM control signal. The proposed method has the advantage that it can be applied in PV systems operating under partial shading conditions. Also, knowledge of either the operational characteristics and configuration of the PV modules within the PV array or the power converter operational characteristics, is not required for its application. The experimental results validated that by using the proposed method, the power production of the PV system is increased significantly compared to the case that only the power production of the PV array is maximized by using a global MPPT technique without tracking the optimal value of the power converter efficiency.

*Index Terms*—Maximum power point tracking (MPPT), optimization, partial shading, photovoltaic (PV) systems, power converter efficiency.

## I. INTRODUCTION

**D**UE to the continuously growing economic competiveness of photovoltaic (PV) technology, the installation of PV systems across the world followed an exponential increase during the last years. Among the global solar installations, the residential PV systems achieved high penetration rates. In Europe, more than two thirds of PV systems were installed on the roofs of residential, commercial, and industrial buildings in 2016 [1]. This trend is expected to continue in the following years due to the continuous evolution of building integrated PV systems that
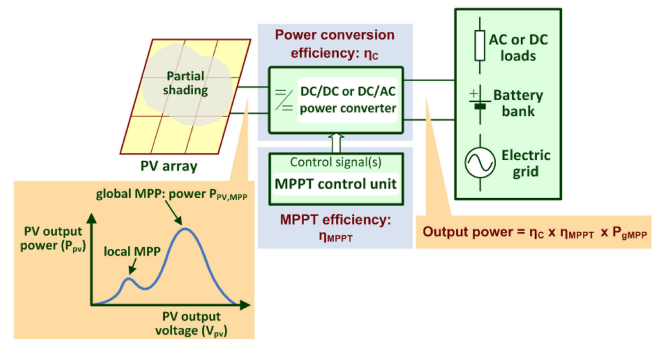
Fig. 1. Generalized block diagram of a residential PV system.

facilitate the implementation of nearly zero-energy buildings according to the European Union policy requirements.

A generalized block diagram of a residential PV system is shown in Fig. 1. It consists of a PV array with multiple PV modules connected in series and/or parallel and a dc/dc or dc/ac power electronic converter that transfers the energy produced by the PV array to the load (e.g., battery bank, electric grid, etc.). In residential PV applications, the PV modules comprising the PV power generator are highly prone to partial shading caused by nearby buildings, trees, etc. Under these conditions, the individual PV modules of the PV array receive unequal amounts of solar irradiance. This results in the power-voltage characteristic of the PV array to exhibit one or more maximum power points (MPPs) where the PV power is locally maximized (i.e., local MPPs), whereas only one of them corresponds to the global MPP where the maximum possible power is produced by the PV array (i.e., point $P_{\mathrm{PV,MPP}}$ in Fig. 1). The relative position of the global MPP with respect to the local MPP(s) on the power-voltage curve of the PV array, changes continuously during the PV system operation depending on the meteorological and partial shading conditions that prevail at each time instant. For that purpose, the PV system comprises a control unit that performs a maximum power point tracking (MPPT) process in order to control the power converter such that the PV array always operates at the global MPP.

A wide variety of different MPPT methods have been developed in the past for maximizing the power production of PV

arrays either under uniform or non-uniform (i.e., partial shading) incident solar irradiation conditions. Evolutionary algorithms, which in some cases have been inspired by natural or biological processes, have been applied in order to track the global MPP of PV arrays, such as the Grey Wolf optimization algorithm [2], the Firefly algorithm [3], the Particle swarm optimization (PSO) algorithm [4], the Flower Pollination algorithm [5], the Sine Cosine optimization algorithm combined with the Cauchy and Gaussian distributions [6], as well as the "Jaya" [7] and Differential Evolution [8], [9] optimization algorithms. In [10], the Fireworks Algorithm is applied for detecting the position of the global MPP. Mathematical models of a PV string/array under partial shading conditions are used in [11]–[13] for predicting the region where the global MPP resides on the power-voltage characteristic of the PV source. A mathematical model of the PV modules together with an optical camera, which acquires images enabling the estimation of the irradiance received by the PV cells, are used in [14] for calculating the position of the global MPP. PV-model-based MPPT techniques have the disadvantage that knowledge of the PV modules operational characteristics is required for their implementation. However, such information is not available in industrial PV power converter products, where the MPPT control units are integrated, since the specifications of the PV array are determined by the PV system designer after the power converter and the associated MPPT control unit has already been manufactured. Instead of a mathematical model, an artificial neural network can be used for initially deriving a voltage range where the global MPP is located and then apply the perturb and observe (P&O) MPPT method for converging to the global MPP [15]. This method requires the use of a large set of training data, as well as real-time measurements of solar irradiation on the individual PV modules of the array.

The impact of partial shading can be reduced by employing distributed MPPT (DMPPT) systems (e.g., [16]–[18]), where a separate dc/dc or dc/ac power converter with MPPT capability is attached at the individual PV modules of the PV array. However, local MPPs can appear at the output power versus voltage characteristic of the PV modules also in DMPPT systems in case of either partial-shading or non-uniform aging of the individual solar cells that have been encapsulated within the same PV module [14]. The reconfiguration of the electrical connections between the PV modules comprising a PV array, in case of partial-shading or non-uniform aging of the individual solar cells that comprise the PV source, has been proposed in the past for increasing the PV power production under such operating conditions [19], [20]. As an example, the PV array reconfiguration method [21] has the disadvantage of high implementation complexity due to the high number of controllable power switches that must be installed in order to modify the connections among the individual PV modules of the PV array. Moreover, depending on the PV array structure, the partial-shading pattern and the aging rates of the individual solar cells, the power-voltage curve of the PV array may still exhibit local maxima after its reconfiguration. Thus, both in DMPPT and PV-array-reconfigurable PV systems, the use of a global MPPT algorithm capable to maximize the PV array output power is indispensable.

All of the aforementioned global MPPT techniques target to maximize the power production of the PV array under the continuously changing solar irradiation, ambient temperature, and partial-shading conditions by modifying the duty cycle or reference input voltage of a power converter which processes the PV-generated energy. However, the power produced by the PV system at the output of the power converter (see Fig. 1), $P_o$ (W) is given as follows:

$$P_o = \eta_C \cdot \eta_{\mathrm{MPPT}} \cdot P_{g\mathrm{MPP}} \qquad (1)$$

where $\eta_C$ (%) is the efficiency of the power converter, $\eta_{\mathrm{MPPT}}$ (%) is the efficiency of the MPPT control method that is applied to track the global MPP, and $P_{g\mathrm{MPP}}$ (W) is the power of the global MPP of the PV array at each time instant.

The efficiency $\eta_C$ of the power converter depends on its circuit topology and the values of the passive and active components that it comprises, as well as on the switching frequency and the input/output voltage and power levels. Although the circuit topology and components of the power converter remain fixed during the PV system operation, the dc input voltage and power levels vary continuously according to the meteorological conditions and shading pattern of the PV source. Thus, the maximization of the power produced by the PV source through an MPPT process does not guarantee that the maximum amount of power will also be transferred to the load of the power converter. However, considering (1), it is concluded that the power transferred by the PV system to the load can be further increased by dynamically maximizing the efficiency of the power converter in real time under the continuously changing meteorological and partial-shading conditions.

In order to maximize the energy transferred to the load, in [22], it is proposed to track the output power of the dc/dc converter, instead of the input (i.e., PV source) power that is performed by the conventional PV MPPT systems. However, through this approach, the efficiency of the dc/dc converter [i.e., $\eta_C$ in (1)] is not maximized and, therefore, the maximum possible energy is not produced by the PV system. Considering that a high switching frequency reduces the efficiency of the power converter due to higher switching power losses, measurements of solar irradiance are used in [23] in order to reduce the switching frequency of a boost-type dc/dc converter as the solar irradiation and the power produced by the PV source are increased. The duty cycle of the dc/dc converter control signal is determined by executing the P&O MPPT algorithm. This control method has the disadvantage that the switching frequency adaption algorithm does not take into account the impact of ambient temperature on the power production of the PV modules, which, in low latitude installation sites or in building-integrated PV applications, is significant. Additionally, it is not suitable for application in PV arrays subject to non-uniform incident solar irradiation conditions due to partial shading, since in such cases the power-voltage characteristic of the PV source exhibits multiple local MPPs and the P&O MPPT algorithm employed cannot guarantee convergence to the global MPP.

In [24], the P&O algorithm is applied for detecting the switching frequency value where the maximum efficiency is

exhibited by a buck–boost converter that is employed in a module-integrated converter of a PV system. An MPPT algorithm for maximizing the energy production of the PV source has not been incorporated in that control technique. In [25], the switching frequency of a flyback-type dc/dc converter, which is employed in a PV microinverter, is increased linearly with the output power of the microinverter when the dc/dc converter operates in discontinuous conduction mode. Therefore, the switching losses of the dc/dc converter are reduced and the overall microinverter efficiency is increased. In this scheme, the MPPT operation is implemented separately by adjusting the amplitude of the reference current of the controller that regulates the dc/dc converter operation.

One of the two interleaving phases of a PV flyback-type dc/dc converter is disabled in [26] when the operating power level drops below a certain threshold, in order to reduce the switching and core losses of the dc/dc converter. That threshold is calculated by using a model of the microinverter power losses as a function of the input/output voltage levels and output power, respectively, such that the efficiency of the dc/dc converter is maximized. An MPPT algorithm is also executed in parallel with the aforementioned process, in order to maximize the energy production of the PV source. For low-power PV applications, the optimal value of the inductor current in a boost-type dc/dc converter operating in burst mode is calculated in [27] such that the power converter exhibits maximum efficiency irrespectively of the input power level. This technique is not suitable for PV systems with PWM-controlled converters where the power converter is active continuously.

In [28], the MPPT process of a PV microinverter, which consists of a dc/dc converter and a dc/ac inverter, is performed by using the dc/dc converter duty cycle as a control variable. Simultaneously, a maximum efficiency tracking control algorithm is executed in real time where the switching frequency of the dc/dc converter, as well as the switching frequency and dc-bus voltage of the dc/ac inverter, are used as control variables and they are modified according to a gradient-ascent method until convergence to an operating point has been achieved where the efficiency of the overall microinverter has been maximized. This method is not suitable for application in PV arrays subject to partial shading, due to the inability of the gradient-ascent optimization algorithm to avoid convergence to local MPPs.

A dual-pole switching method for a synchronous buck–boost dc/dc converter is proposed in [29], targeting to reduce the core loss of the power converter inductor, which comprises the major part of the converter total power loss, under low power levels. The dual-pole switching method includes a maximum efficiency tracking algorithm for deriving the optimal values of the duty cycles of the control signals driving each pole of the power converter, such that the inductor current ripple is adjusted to a value maximizing the power converter efficiency.

A control method has been proposed in [30] for islanded PV systems that comprise multiple PV sources connected in parallel, where the optimal distribution of the power produced by the power converter of each PV source is calculated by using the Lagrange multiplier method such that the efficiency of the overall power supply system is maximized. However, in order to apply this method, the variation of the power converter efficiency with the input/output voltage and power must be known. Thus, the application of an experimental characterization process of the power converter efficiency is required. A maximum efficiency tracking algorithm for PV systems comprising multiple dc/ac inverters operating in parallel is proposed in [31], but knowledge of the efficiency characteristics of the PV inverters is also required for its implementation. In order to increase the overall efficiency of grid-connected PV systems comprising multiple module-integrated converters connected in parallel to a common dc bus, it is proposed in [32] to pause the switching operation of the dc/dc converter where the maximum MPP voltage value has been developed and directly connect the corresponding PV module to the dc bus through a diode. Therefore, the switching losses of that power converter are eliminated and the energy production of the overall PV system can be increased. The MPPT process of the PV module connected to the disabled power converter is achieved by regulating the dc bus voltage through a dc/ac inverter. The rest of the module-integrated power converters continue the execution of the MPPT process without interruption.

Efficiency optimization methods have also been developed for power converters that do not operate with a PV input power source. An online efficiency optimization technique for dual-active-bridge converters has been presented in [33]. An optimization controller calculates the optimal duty cycle value of one of the two half-bridges, as well as the optimal value of the mutual phase shift of the two half-bridge legs of the converter, by using the simplex optimization algorithm, such that the converter operates at the maximum efficiency point. The second half-bridge duty cycle is used to control the power converter output voltage. The optimal switching frequency values of a flyback-type dc/dc power converter, which have been previously calculated offline according to an optimal design process using a power loss model of the converter for various input voltage and current operating conditions, are stored in a lookup table in [34]. The lookup table is programmed in a digital controller and it is used in real time for achieving operation of the power converter at the maximum efficiency point. A gradient-ascent optimization algorithm is applied in [35] for tracking the maximum efficiency point of an isolated half-bridge dc/dc converter with current doubler, by iteratively modifying the power switches dead time that affects the power losses of the switches body diodes. Finally, the topology morphing control is proposed in [36] for increasing the efficiency of an *LLC* resonant dc/dc converter, which operates under wide input and/or output voltage ranges. The topology control is implemented during real-time operation by modifying the power converter circuit structure from full-bridge to half-bridge and vice versa, according to the input and output voltage levels. This technique improves the efficiency versus input voltage characteristic curve of the power converter, but it does not track the overall maximum efficiency point of the power converter.

In this paper, a new control method is proposed for the first time in the existing literature for the real-time maximization of the energy production of PV systems. In the proposed technique, the duty cycle and switching frequency of the power converter
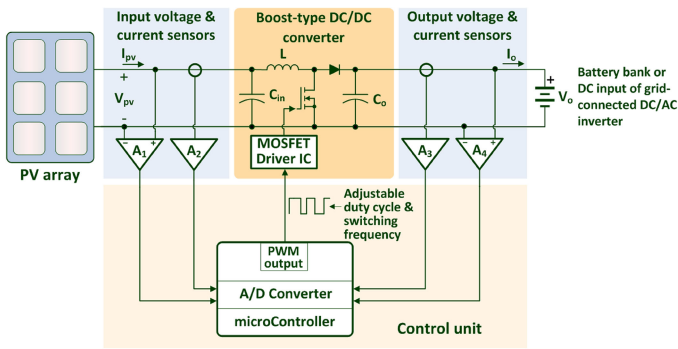
Fig. 2.    Block diagram of the PV system under study.

PWM control signal are used as two independent control variables that are modified in real-time such that the maximum possible power is produced by the PV source and, simultaneously, the maximum power is produced by the power converter of the PV system, under the continuously changing meteorological and partial shading conditions. Compared to the past-proposed techniques described before, the proposed method exhibits the following advantages:

1) maximizes both the energy produced by the PV array and the efficiency of the dc/dc converter, thus achieving the overall maximization of the output power of the PV system;

2) is suitable for application in PV systems operating under partial shading conditions, due to its ability to detect the global MPP of the power converter output-power versus input-voltage characteristic;

3) does not require knowledge of the operational characteristics and configuration of the PV modules within the PV array;

4) does not require knowledge of the power converter operational characteristic (e.g., efficiency curve, power losses of the components, etc.).

As demonstrated by the experimental results that are presented in this paper, the power production of the overall PV system can be increased significantly by applying the proposed control method, compared to the use of a global MPPT algorithm that tracks only the global MPP of the PV array.

The rest of this paper is organized as follows. The operation of the proposed control method is described in Section II. The experimental results from the application of the proposed technique in a PV system are presented in Section III. Finally, conclusions are drawn in Section IV.

## II. PROPOSED CONTROL SYSTEM

A block diagram of the PV system under study is illustrated in Fig. 2. The PV array comprises multiple PV modules connected in series and/or parallel. A boost-type dc/dc converter is used to interface the energy produced by the PV array to a battery bank or to the dc input of a grid-connected dc/ac inverter. The dc/dc converter is designed to operate in the continuous-conduction mode, where the dc input and output voltage levels are related

as follows [37]:

$$V_{\text{pv}} = V_o \cdot (1 - D) \tag{2}$$

where $V_{\text{pv}}$ (V) is the voltage produced by the PV array, $V_o$ (V) is the voltage of the battery bank, and $D$ $(0 < D < 1)$ is the duty cycle of the pulsewidth modulated (PWM) control signal that drives the dc/dc converter power switch (e.g., power MOSFET). Since the value of $V_o$ remains relatively constant over a short time interval of the power converter operation, the dc voltage of the PV array and the corresponding operating point on the power-voltage characteristic of the PV source can be modified by adjusting the value of $D$ in (2).

In the proposed control method, the dc input/output voltage and current of the dc/dc converter are measured by the microcontroller unit in order to control the operation of the dc/dc power converter by producing a PWM control signal with adjustable switching frequency $f_s$ (Hz) and duty cycle $D$, which drives the power switch of the dc/dc converter, such that the following statements hold: first, the maximum possible power is produced by the PV array under the continuously changing solar irradiation and ambient temperature conditions, even in case of partial shading of the PV modules of the PV array, and second, the maximum possible power is produced by the dc/dc converter for each value of input power provided by the PV source. Through these two conditions, the energy efficiency of the overall PV system is continuously maximized in real time.

In case of partial-shading conditions, both the PV power versus voltage characteristic and the dc/dc converter output-power versus input-voltage characteristic exhibit multiple local MPPs. As analyzed in Section I, various different evolutionary optimization algorithms have been applied in the past for detecting the global MPP of a PV array that operates under non-uniform incident solar irradiation conditions [2]–[10]. In this paper, the PSO algorithm has been employed in the proposed method due to its implementation simplicity, low computation requirements, as well as its ability to converge to the global maximum operating point without been trapped in local maxima [4]. However, till present, the PSO algorithm has been employed in prior art (e.g., in [4]) only for maximizing the output power of PV arrays. In these applications, the PSO algorithm has been configured to comprise particles corresponding only to alternative values of the duty cycle of the dc/dc converter control signal. In contrast to prior art, in this paper, the particles of the PSO algorithm have been augmented to consist of $2 \times 1$ vectors, each containing values of both the duty cycle $D$ and the switching frequency $f_s$ of the dc/dc converter PWM control signal. A flowchart of the proposed PSO algorithm for maximizing both the PV array output power and the dc/dc converter output power is depicted in Fig. 3. Initially, a population of particles is generated randomly. Then, the PSO algorithm is executed iteratively. During each iteration, the duty cycle and switching frequency values contained in each particle are applied to the dc/dc converter. The corresponding output power of the converter is calculated by measuring its output voltage and current as follows:

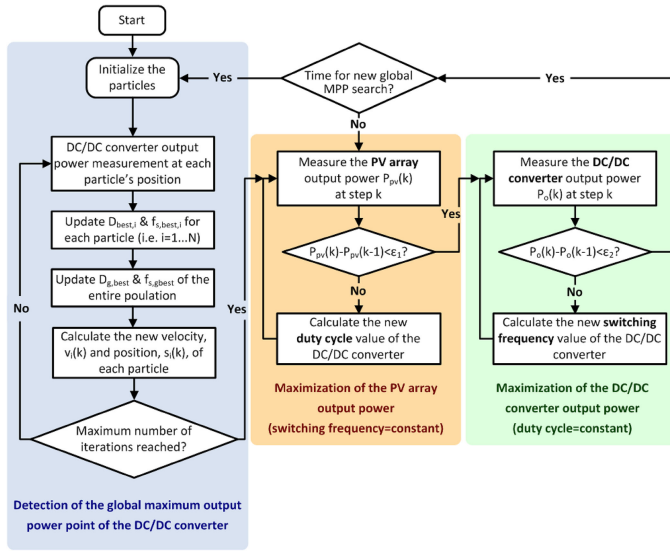$$P_{o,i}(k) = V_{o,i}(k) \cdot I_{o,i}(k) \tag{3}$$

Fig. 3.     Flowchart of the proposed algorithm for maximizing the output power production of a PV system under partial shading conditions.

where $P_{o,i}(k)$ (W) is the dc/dc converter output power and $V_{o,i}(k)$ (V) and $I_{o,i}(k)$ (A) are the measured dc/dc converter output voltage and current, respectively, for the $i$th particle at the $k$th iteration of the control algorithm.

The dc/dc converter output power levels produced by the individual particles are compared and the particle providing the maximum value of dc/dc converter output power is considered as the globally best particle of the overall swarm till that iteration. Then, the position and velocity of each particle are updated as follows:

$$\boldsymbol{s}_i(k) = \begin{bmatrix} D_i(k) \\ f_{s,i}(k) \end{bmatrix} = \begin{bmatrix} D_i(k-1) \\ f_{s,i}(k-1) \end{bmatrix} + \boldsymbol{v}_i(k) \qquad (4)$$

and

$$\begin{aligned}
\boldsymbol{v}_i(k) &= \begin{bmatrix} v_{D,i}(k) \\ v_{f_s,i}(k) \end{bmatrix} = w \cdot \begin{bmatrix} v_{D,i}(k-1) \\ v_{f_s,i}(k-1) \end{bmatrix} \\
&+ fp \cdot rp \cdot \left\{ \begin{bmatrix} D_{\text{best},i} \\ f_{s,\text{best},i} \end{bmatrix} - \begin{bmatrix} D_i(k-1) \\ f_{s,i}(k-1) \end{bmatrix} \right\} \\
&+ fg \cdot rg \cdot \left\{ \begin{bmatrix} D_{g,\text{best}} \\ f_{s,g,\text{best}} \end{bmatrix} - \begin{bmatrix} D_i(k-1) \\ f_{s,i}(k-1) \end{bmatrix} \right\} \quad (5)
\end{aligned}$$

where $\boldsymbol{s}_i(k)$ and $\boldsymbol{v}_i(k)$ are the position and velocity, respectively, of the $i$th particle during the $k$th iteration, $D_i(k)$ [where $0 < D_i(k) < 1$] and $f_{s,i}(k)$ (Hz) are the duty cycle and switching frequency, respectively, of the $i$th particle during the $k$th iteration, $v_{D,i}(k)$ and $v_{f_s,i}(k)$ are the velocity of the duty cycle and switching frequency, respectively, of the $i$th particle during the $k$th iteration, $D_{\text{best},i}$ and $f_{s,\text{best},i}$ are the best duty cycle and switching frequency, respectively, values that have been derived till the $k$th iteration for the $i$th particle and $D_{g,\text{best}}$ and $f_{s,g,\text{best}}$ are the best duty cycle and switching frequency, respectively, values that have been derived till the $k$th iteration for the entire population.

The values of $w$, $f_p$, and $f_g$ are constant during the execution of the PSO algorithm, whereas new, random, values of $r_p$ and $r_g$ are produced during each iteration according to the uniform distribution. The process described before is repeated till a predefined number of iterations have been performed. During these iterations, the entire population of particles progressively moves toward the direction (i.e., the combination of duty cycle and switching frequency values), which result in the maximum possible power to be produced by the dc/dc converter of the PV system. The PSO-based algorithm enables to derive the values of duty cycle and switching frequency that result in the maximization of the power produced by the dc/dc power converter even if the output-power versus input-voltage characteristic of the power converter exhibits one or more local MPPs in case of PV array operation under partial-shading conditions.

After convergence to the global maximum output power point of the dc/dc converter, the duty cycle and switching frequency are continuously adjusted independently in order to continuously track any small movements of the global maximum output power point position, which are caused by short-term changes of the incident solar irradiation and/or shading pattern that do not alter the relative position and/or strength of the global MPP compared to the local MPPs. Thus, the operation of the PV system at the global maximum output power point previously detected by the PSO-based algorithm can be maintained. Through this approach, the entire output-power versus input-voltage characteristic of the dc/dc converter is not re-examined, thus avoiding any power loss that would result when operating at points away from the global maximum output power point. As shown in Fig. 3, during that process, the PV array MPP is initially re-tracked by adjusting the duty cycle of the dc/dc converter control signal according to the conventional P&O algorithm. During this process, the PV array output power levels produced at subsequent iterations are compared and the dc/dc converter duty cycle is modified according to the following control law:

$$\begin{aligned}
D(k) = D(k-1) &+ C_1 \cdot \text{sign}\left(D(k-1) - D(k-2)\right) \\
&\cdot \text{sign}\left(P_{\text{pv}}(k-1) - P_{\text{pv}}(k-2)\right) \quad (6)
\end{aligned}$$

where $D(k)$ and $P_{pv}(k)$ (W) are the values of the dc/dc converter duty cycle and PV array output power, respectively, at step $k$, $C_1$ is a constant and the function $\text{sign}(\cdot)$ is defined as follows:

$$\text{sign}(x) = \begin{cases} 1 & \text{if } x \geq 0 \\ 0 & \text{if } x < 0. \end{cases} \qquad (7)$$

The power produced by the PV array in (6) is calculated by measuring the output voltage and current of the PV array

$$P_{\text{pv}}(k) = V_{\text{pv}}(k) \cdot I_{\text{pv}}(k) \qquad (8)$$

where $V_{pv}(k)$ (V) and $I_{pv}(k)$ (A) are the measured PV array output voltage and current, respectively, at the $k$th iteration of the control algorithm.

The above-mentioned process is repeated till the difference of PV array output power levels produced at subsequent iterations is less than a predefined threshold (i.e., parameter $\varepsilon_1$ in Fig. 3). Then, the dc/dc converter maximum output power is re-tracked. For that purpose, the switching frequency is

adjusted by comparing the dc/dc converter output power values that result before and after a change of switching frequency has been applied. If the new output power level of the dc/dc converter is higher, then the switching frequency change is continued toward the same direction, else the direction of changes is reversed. Thus, the switching frequency adjustment is performed according to the following control law:

$$f_s(k) = f_s(k-1) + C_2 \cdot \text{sign}\left(f_s(k-1) - f_s(k-2)\right)$$
$$\cdot \text{sign}\left(P_o(k-1) - P_o(k-2)\right) \qquad (9)$$

where $f_s(k)$ (Hz) and $P_o(k)$ (W) are the values of switching frequency and dc/dc converter output power, respectively, at step $k$ and $C_2$ is a constant.

This process of tracking the dc/dc converter maximum output power point is continued till the difference of the dc/dc converter output power levels that are produced at subsequent iterations is less than a predefined threshold (i.e., parameter $\varepsilon_2$ in Fig. 3). During the duty-cycle regulation stage, the switching frequency value remains constant, whereas during the switching frequency adjustment phase, the duty cycle value is not altered, thus maintaining the power produced by the PV array to the previously detected MPP.

During the execution of all stages of the proposed algorithm (see Fig. 3), the time interval between subsequent perturbations of the dc/dc converter duty-cycle and switching frequency is selected to be higher than the settling time of the dc/dc converter output power (typically a few milliseconds) in order to ensure stable operation of the overall PV system [38].

In typical residential applications of PV systems, partial shading is caused by objects (e.g., buildings, poles, trees, etc.) located next to the PV array. Since the position of such shading objects is constant, the resulting pattern of partial shading on the surface of the PV array changes due to the movement of the sun and its rate of change is low. Thus, in the proposed method, the PSO-based algorithm is automatically re-initiated with a time period of several minutes in order to detect the values of duty cycle and switching frequency corresponding to the new global maximum output power point of the dc/dc converter. The total time required for the PSO-based part of the proposed algorithm (see Fig. 3) to detect the global MPP of the dc/dc converter output power is a few seconds. Therefore, due to the periodic re-execution of the PSO algorithm with a time period of the order of several minutes, as mentioned before, the curve scanning process results in insignificant energy loss while simultaneously retaining the advantage of the proposed method, compared to model-based MPPT methods, of not requiring knowledge of the PV array operational characteristics.

During the execution of the PSO algorithm, the switching frequency of the dc/dc converter $f_s$ is allowed to be modified within a predefined range of lower and upper bounds $[f_{s,\min}, f_{s,\max}]$. The value of the input capacitor $C_{\text{in}}$ of the dc/dc converter (see Fig. 2) should be calculated according to the minimum possible value of switching frequency, $f_{s,\min}$, according to [37] such that the ripple of the PV array output voltage is minimized in order to avoid the corresponding energy loss [38]. In case of battery charging applications, the output capacitance $C_o$ of the dc/dc converter (see Fig. 2) should be large enough to minimize the ripple current of the battery bank, in order to avoid the degradation of its lifetime. If the output of the dc/dc converter is connected to the dc input of a grid-connected dc/ac inverter, then the value of $C_o$ should be calculated as discussed in [38] for decoupling the dc/dc and dc/ac stages of the PV system.

As a first step of development and implementation, the proposed method has been applied in a boost-type dc/dc converter, which is frequently employed both in low-power PV systems for battery charging applications [27] and in grid-connected centralized or DMPPT PV systems [39], due to the simplicity of its circuit structure and easy control. However, it can also be applied in PV dc/dc or dc/ac power converters with alternative topologies [18], [39]–[41].

The target of the proposed method is to optimize the real-time operation of the PV array and dc/dc conversion stages of the PV system. In case of battery charging applications where a battery bank is connected to the output of the dc/dc converter, the battery voltage remains relatively constant during the MPPT process execution without affecting its performance [6]. The battery voltage can be regulated to the desired value by incorporating a separate battery-charging controller (e.g., based on the algorithm presented in [42]). In case of cascade dc/dc–dc/ac PV systems, the dc-link voltage (i.e., corresponding to $V_o$ in Fig. 2) is regulated by the controller of the dc/ac inverter (e.g., as analyzed in [43] and [44]). In these PV system topologies, the dc-link voltage regulation can also take into account the maximization of the dc/ac inverter efficiency by considering the corresponding techniques of prior art that were described in Section I and, therefore, in combination with the proposed technique, achieve the optimization of the energy production performance of the overall PV system. Both the battery-charging control and the dc-link voltage regulation processes are not within the scope of the work proposed in this paper.

Till present, DMPPT systems have been employed for reducing the impact of partial shading by tracking the MPP of the individual PV modules of the PV source. As mentioned in Section I, local MPPs can also appear at the output power versus voltage characteristic of the PV modules in DMPPT architectures. Therefore, the proposed method is also applicable in PV systems employing the DMPPT architecture in order to track the global MPP of each PV module and, simultaneously, maximize the efficiency of the corresponding dc/dc or dc/ac converter.

## III. EXPERIMENTAL RESULTS

The performance of the proposed method has been evaluated outdoors under real operating conditions. For that purpose, a fully functional experimental prototype of the PV system illustrated in Fig. 2 has been developed, which is depicted in Fig. 4.

The PV array comprises two monocrystalline silicon PV modules with bypass diodes, connected in parallel. The specifications of the PV modules provided by the manufacturer under standard test conditions (STC) are presented in Table I. A boost-type dc/dc converter has been built using an $L = 100\ \mu\text{H}$ inductor, a $C_o = 3$ mF output capacitor, as well as the STTH61W04SW diode and the PSMN2R2-40PS power MOSFET. The PV-generated energy is transferred to a 12-V battery bank consisting of two 7-Ah lead-acid batteries connected in
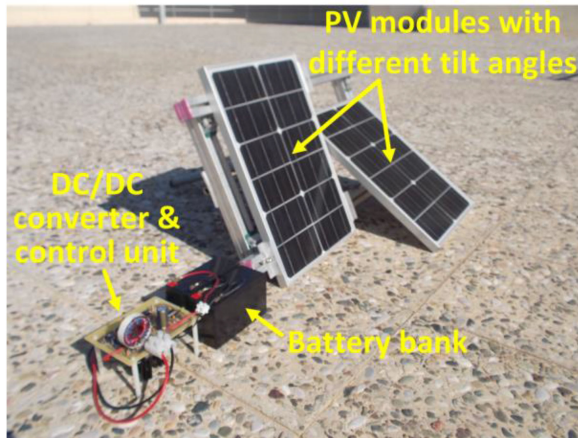
Fig. 4.    Experimental prototype PV system that was developed for evaluating the performance of the proposed method under real operating conditions.

TABLE I
SPECIFICATIONS OF THE PV MODULES UNDER STC

| Open-circuit voltage | 7.02 V |
|---|---|
| Short-circuit current | 3.4 A |
| MPP power | 20 W |

parallel. The proposed algorithm has been programmed for execution by the Atmel ATMEGA328P-PU microcontroller, which features an on-chip six-channel and 10-bit analog-to-digital converter. The dc input and output currents of the power converter have been measured by using the ACS712 Hall effect sensors. The dc input and output voltages have been measured with resistive voltage dividers interfaced to voltage-followers based on operational amplifiers.

The PSO-based part of the algorithm was implemented with a population of 10 particles and it was programmed to be executed for 20 generations every 5 min. Additionally, the values of $w = 0.3$, $f_p = 1.8$, and $f_g = 1.3$ were applied in (5) and the values of $C_1$ and $C_2$ in (6) and (9), respectively, have been set equal to 3% and 5 kHz, respectively. These values, together with the number of particles and the number of generations, were selected after performing various trial-and-error experimental tests, such that the search process for maximizing the dc/dc converter output power is accomplished with the minimum number of search steps, thus speeding-up the convergence of the tracking process. This process is based on measurements of the input–output behavior of the PV system (i.e., output power of the PV array versus dc/dc converter output power production), without requiring any prior knowledge of its internal structure (e.g., characterization of the PV modules current–voltage curve, measurement of the dc/dc converter components operating characteristics, etc.).

The target of the proposed control method is to maximize the power production of the overall PV system. According to the experimental setup depicted in Fig. 4, the PV modules comprising the overall PV array were installed with different tilt angles such that they receive unequal amounts of solar irradiance, in
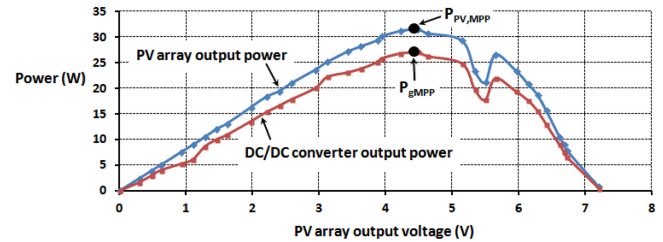


Fig. 5.    PV array and the dc/dc converter output power versus the PV array output voltage in case that $f_s = 100$ kHz and the global MPP is located at a lower voltage compared to the local MPP.

order to emulate partial-shading conditions on the surface of the PV array and investigate the performance of the proposed technique with different shapes of the PV array output power versus voltage characteristic, as described ahead. Therefore, initially, the tilt angles of the two PV modules comprising the PV array were set such that the global MPP is located at a lower voltage compared to the local MPP on the output-power versus input-voltage characteristic of the dc/dc converter. The resulting, experimentally measured, power that is produced by the PV array and the dc/dc converter over the entire dc input voltage range produced by the PV array when the dc/dc converter switching frequency has been set constant and equal to $f_s = 100$ kHz (i.e., without executing the proposed maximization process) is illustrated in Fig. 5. This benchmark switching-frequency value has been selected similarly to [3] (where, however, only the MPP of the PV source is tracked) and enables to reduce the size of the inductor $L$ (see Fig. 2) and, consequently, to reduce the volume and cost of the dc/dc power converter [37]. It is observed that due to the incidence of non-uniform solar irradiance levels on the individual PV modules of the PV array, the output-power versus input-voltage characteristic of the dc/dc converter also exhibits a local MPP, as well as a global MPP where the output power is maximized (i.e., 27.1 W at point $P_{g\mathrm{MPP}}$ in Fig. 5). As shown in Fig. 5, the maximum power that can be extracted by the overall PV array that is connected to the dc/dc converter (see Fig. 2) in the considered experimental set-up is equal to $P_{\mathrm{PV,MPP}} = 31.51$ W. Then, the PSO-based part of the proposed algorithm was executed. The power produced by the PV array and the dc/dc converter, respectively, according to all of the duty cycle and switching frequency values explored by the PSO algorithm during its execution (i.e., contained in each particle of each of the 20 generations of execution of the PSO algorithm, which resulted in 200 different search steps) are depicted in Fig. 6(a) and (b). The corresponding values of the PV array output voltage and the dc/dc converter efficiency, duty cycle, and switching frequency are presented in Fig. 6(c)–(f).

It is observed that during the evolution of the PSO process, both the duty cycle and switching frequency of the dc/dc converter are concurrently modified [see Fig. 6(e)–(f)], which affects both the power produced by the PV array and the efficiency of the dc/dc converter, respectively [see Fig. 6(a) and (d)]. Due to the random initialization of most of the particles positions away from the maximum output power point, the dc/dc converter operates initially with non-optimal values of duty cycle and switching frequency, which resulted in a substantial reduction of the dc/dc converter output power at step 1. However,
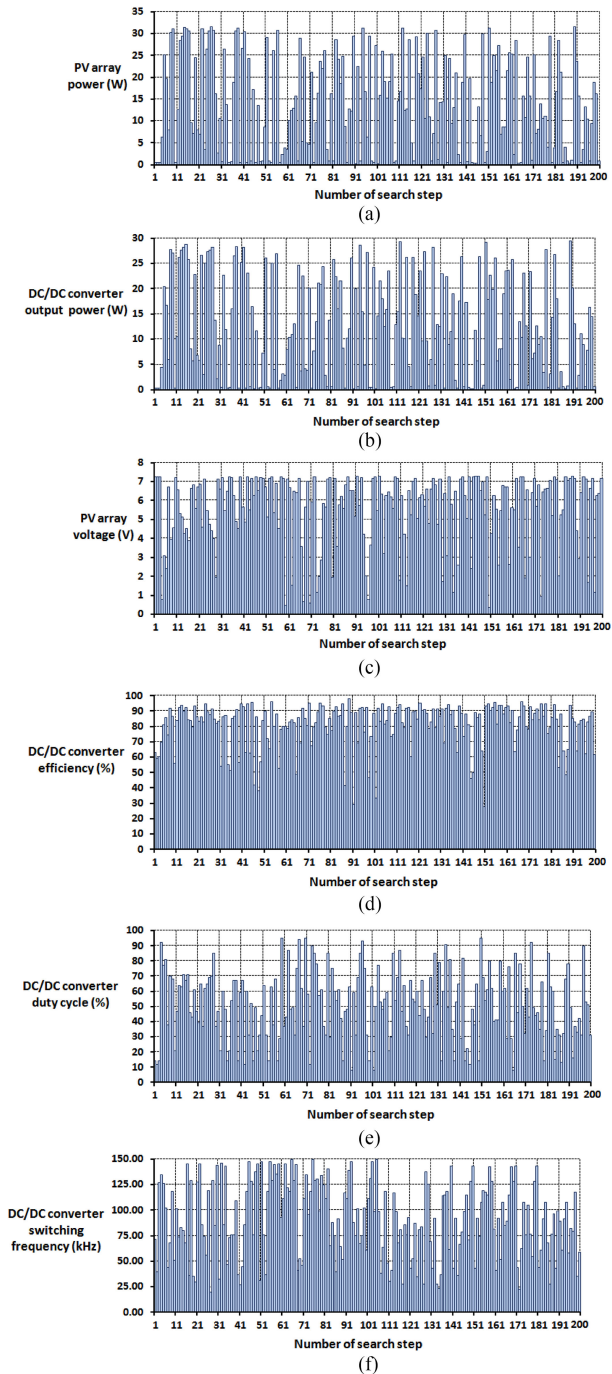
Fig. 6. Operation of the dc/dc converter during the PSO algorithm execution in case that the global MPP is located at a lower voltage compared to the local MPP. (a) PV array output power. (b) DC/DC converter output power. (c) PV array output voltage. (d) DC/DC converter efficiency. (e) Duty cycle. (f) Switching frequency.
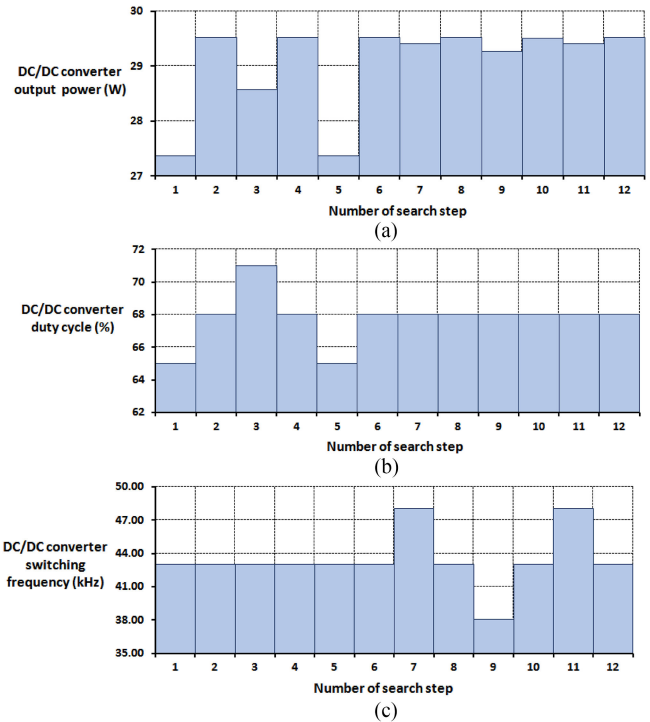


Fig. 7. Maximization of the dc/dc converter output power after the PSO algorithm execution, in case that the global MPP is located at a lower voltage compared to the local MPP. (a) DC/DC converter output power. (b) Duty cycle. (c) Switching frequency.

during the evolution of the search process, the PSO particles progressively detect the operating point where the output power of the dc/dc converter is maximized. Thus, at search step 189, which belongs in the 19th generation of the PSO algorithm evolution, the best particle of the swarm contains the duty cycle and switching frequency values of 68.0% and 43.03 kHz, respectively, which result in operation of the PV array at the global MPP [i.e., point $P_{\mathrm{PV,MPP}} = 31.51$ W in Figs. 4 and 5(a), respectively] and, simultaneously, the production of 29.52 W by

the dc/dc converter, which is the maximum output power level derived during the entire evolution of the PSO algorithm (i.e., 200 different search steps over 20 generations). When the execution of the PSO-based process has been accomplished at search step 200 of Fig. 6, the parts of the proposed algorithm, which perform a local-search process for maximizing the PV array output power (by modifying the dc/dc converter duty cycle) and maximizing the dc/dc converter output power (by modifying the dc/dc converter switching frequency), respectively, are executed. This local-search process starts from the optimal operating point $D_{g,\mathrm{best}} = 68.0\%$, $f_{s,g,\mathrm{best}} = 43.03$ kHz, which was previously detected by the PSO algorithm. The variation of the dc/dc converter output power, duty cycle, and switching frequency during that time interval is shown in Fig. 7.

During steps 1–6 the duty cycle of the dc/dc converter is modified in order to search for a better operating point, in terms of the PV system power production than that previously derived by the PSO algorithm (e.g., due to an abrupt change of the meteorological conditions) while keeping the dc/dc converter switching frequency to a constant value. When this process has been finished at step 6, the duty cycle is kept constant and the switching frequency is progressively modified [i.e., during steps 7–12 in Fig. 7(c)] in order to search for potentially better switching frequency values that result in higher output power of the dc/dc converter than the switching frequency derived by the PSO algorithm (e.g., due to a change of the PV array output power and voltage during the aforementioned duty-cycle tuning process). After step 12, the duty-cycle and switching frequency re-adjustment process is repeated for maintaining the dc/dc converter output power to the previously detected optimal
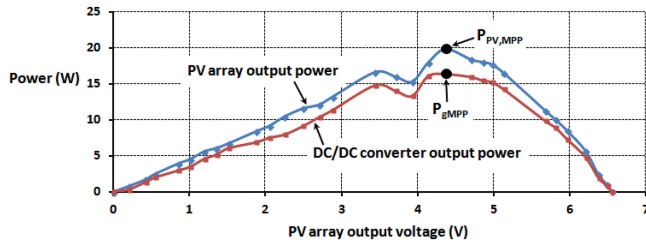
Fig. 8.    PV array and the dc/dc converter output power versus the PV array output voltage in case that $f_s = 100$ kHz and the global MPP is located at a higher voltage compared to the local MPP.

value of $P_{gMPP} = 29.52$ W, till the PSO algorithm is reactivated as described in Section II for performing a new global search process. The resulting optimal value of 29.52 W that is produced by the dc/dc converter is higher by 8.93% compared to the case that the switching frequency of the dc/dc converter is constant at 100 kHz and only the MPPT process of the PV source is executed for operation at the global MPP point (i.e., point $P_{gMPP} = 27.1$ W in Fig. 5, as performed by the existing global MPPT techniques [2]–[15]).

The performance of the proposed method was also tested for different relative positions of the global and local MPPs. For that purpose, the tilt angles of the PV modules were changed in order to alter the amount of solar irradiation incident on each PV module, such that the global MPP is now located at a higher voltage compared to the local MPP on the output-power versus input-voltage characteristic of the dc/dc converter. The resulting, experimentally measured, power that is produced by the PV array and the dc/dc converter over the entire dc output voltage range of the PV array, when the dc/dc converter switching frequency has been set constant at 100 kHz, is plotted in Fig. 8.

It is observed that in this experimental set-up, the maximum power that can be extracted by the overall PV array, which is connected to the DC/DC converter, is equal to $P_{PV,MPP} = 19.89$ W. The power produced by the PV array and the dc/dc converter, respectively, according to all of the duty cycle and switching frequency values explored by the PSO algorithm during its execution (i.e., contained in each particle of the 20 generations of the PSO algorithm execution), are depicted in Fig. 9(a) and (b). The corresponding values of the PV array output voltage and the dc/dc converter efficiency, duty cycle, and switching frequency, are presented in Fig. 9(c)–(f). Similarly to the previous test, during the evolution of the PSO algorithm, the dc/dc converter duty cycle and switching frequency are concurrently and continuously modified, which affects both the power produced by the PV array and the efficiency of the dc/dc converter. The maximum output power of the dc/dc converter is equal to 18.18 W and it is detected by a PSO particle at search step 90 [see Fig. 9(b)] for the duty cycle and switching frequency values of 67.0% and 57.88 kHz, respectively [see Fig. 8(e) and (f)]. At that operating point, the corresponding output power of the PV array [see Fig. 9(a)] is equal to 19.25 W, which deviates by 3.22% from the power level of $P_{PV,MPP} = 19.89$ W of the corresponding global MPP of the PV array depicted in Fig. 8. This deviation is due to the
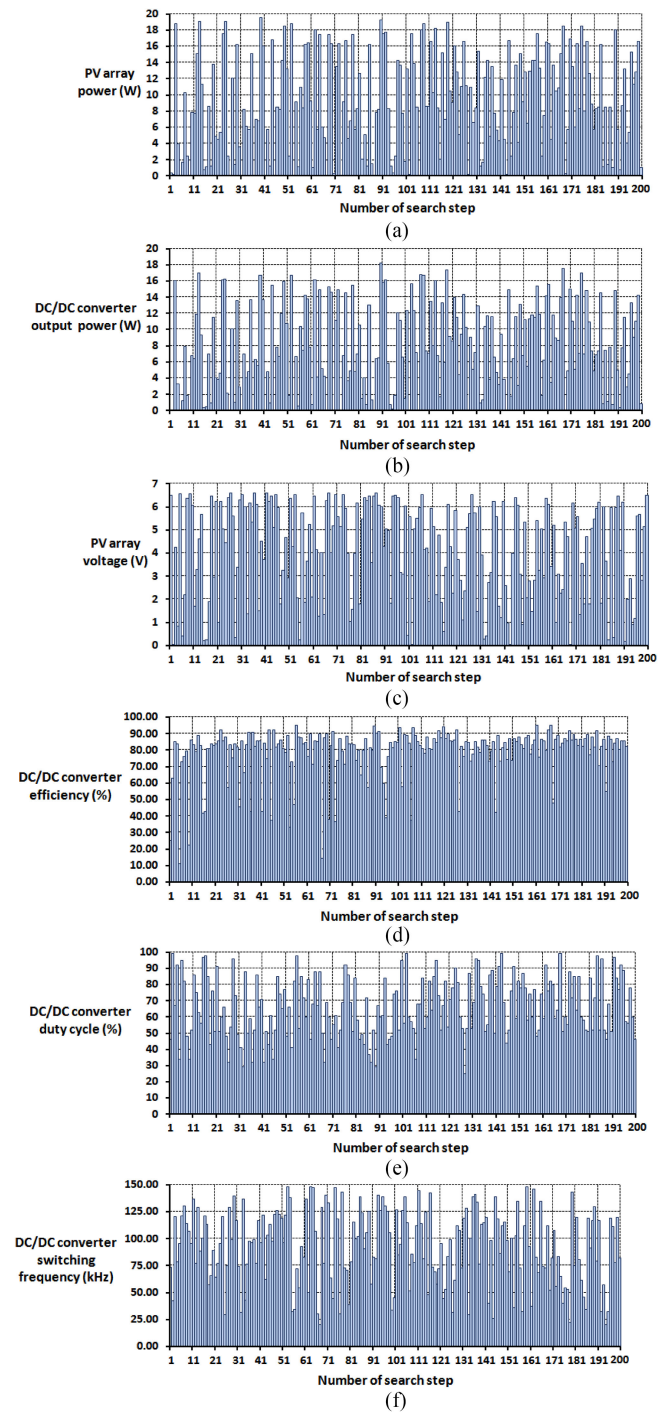


Fig. 9.    Operation of the dc/dc converter during the PSO algorithm execution in case that the global MPP is located at a higher voltage compared to the local MPP. (a) PV array output power. (b) DC/DC converter output power. (c) PV array output voltage. (d) DC/DC converter efficiency. (e) Duty cycle. (f) Switching frequency.

slight change of the meteorological conditions during the time interval between the scanning of the PV array output power characteristic (shown in Fig. 8 and conducted only for performance evaluation purposes) and the application of the proposed PSO search process presented in Fig. 9. This is demonstrated in the experimental results presented in Fig. 10, which were derived when the parts of the proposed algorithm maximizing the dc/dc
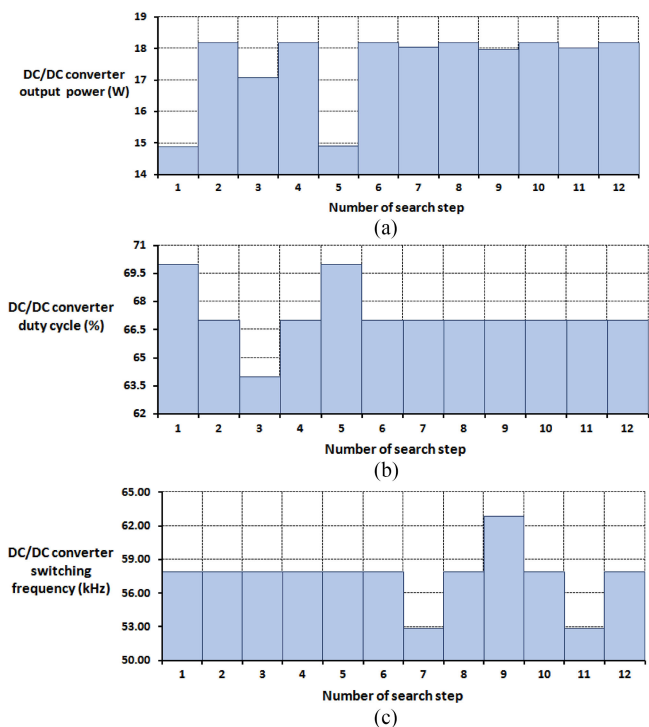
Fig. 10. Maximization of the dc/dc converter output power after the PSO algorithm execution, in case that the global MPP is located at a higher voltage compared to the local MPP. (a) DC/DC converter output power. (b) Duty cycle. (c) Switching frequency.

converter output power by tuning the dc/dc converter duty cycle and switching frequency, respectively, were executed, after the PSO-based maximization process terminated (at search step 200 in Fig. 9). This local-search process started from the operating point $D_{g,\text{best}} = 67.0\%$, $f_{s,g,\text{best}} = 57.88$ kHz derived initially by the PSO algorithm. The values of the dc/dc converter output power, duty cycle and switching frequency during each search step of the local-search process are shown in Fig. 10. It is observed that the variation of the dc/dc converter duty cycle according to (6) during search steps 1–6 and then the modification of the switching frequency by following (9) during search steps 7–12, resulted in the verification that the operating point $D_{g,\text{best}} = 67.0\%$, $f_{s,g,\text{best}} = 57.88$ kHz initially detected by the PSO algorithm is the optimal one for the meteorological conditions prevailing at that time instant. The resulting maximum output power of the dc/dc converter is equal to 18.18 W, which is higher by 10.72% compared to the power production at the operating point derived when the switching frequency is constant at 100 kHz and only a global MPPT process of the PV array is executed (i.e., point $P_{g\text{MPP}} = 16.42$ W in Fig. 8 as performed by the conventional global MPPT techniques [2]–[15]). This local-search process is repeated (according to Fig. 3) in order to compensate any global MPP movement due to short-term changes of the meteorological or shading conditions, which alter the shape of the PV array output power versus voltage characteristic, such that the maximum possible power is continuously produced by the dc/dc converter, till the PSO search process is re-initiated, as described before.

The PSO-based optimization algorithm enables to derive the optimal values of duty cycle and switching frequency with a relatively small number of particles and generations, which resulted in operation of the PV array at $20 \times 10 = 200$ different operating points during the evolution of the proposed maximization process. An exhaustive-search algorithm, scanning the entire search space with a 3% duty cycle step in the range of 36%–93% and a 5-kHz switching-frequency step over the 20–150-kHz range, which were applied in the experimental results presented before, would require operation of the PV system at 540 different operating points. Thus, the proposed PSO-based algorithm effectively reduces the time required to derive the global optimum operating point of the PV system (by 62.96% in the previous experimental tests), as well as the associated power loss due to operation away from the global maximum output power point during the search process.

The sets of optimal values of duty cycle and switching frequency, which have been derived at the last steps of the experimental tests presented in Figs. 5, 6, 8, and 9, respectively, are different and they are in the ranges of 67.0%–68.0% and 43.03–57.88 kHz, respectively. This is due to the different levels of output power and voltage produced by the PV array in each of these experiments, as shown in Figs. 4 and 7, respectively, which affect both the MPP power and MPP voltage of the PV source and the efficiency of the dc/dc converter. As an example of the energy production benefit offered by the ability to automatically modify the switching frequency and track its new optimal value, it has been measured experimentally that for the test conditions of Figs. 7–9, by increasing the switching frequency from 49.94 to 57.88 kHz increases the efficiency of the dc/dc converter by 4.6%. Therefore, it is concluded that depending on the continuously changing partial shading, incident solar irradiance and ambient temperature conditions that prevail, a continuous tracking of different optimal values of duty cycle and switching frequency must be performed in order to maximize the power produced by the dc/dc converter. Furthermore, the experimental tests presented before demonstrate that, in contrast to the corresponding techniques of prior art, the proposed method is capable to maximize the overall output power of the PV power converter without knowledge of the operational characteristics of either the dc/dc converter (e.g., its efficiency curve), or the PV array (e.g., open-circuit voltage, number of PV modules connected in series and/or parallel, etc.). This feature of the proposed technique is important for industrially manufactured PV power converters, where different values of operating power and voltage of the PV source can be applied in each PV application of the same PV power converter product, since the specifications of the PV source are defined by the final PV system designer after the PV power converter has been provided in the market and the operating power and voltage of the PV source are affected by the partial-shading pattern applied (e.g., Figs. 5 and 7), which cannot be known *a priori*. The optimal switching frequency of the PV power converter cannot be known accurately during its design due to the tolerances of the electrical characteristics of the electric and electronic components that it comprises, compared to their datasheet values. Also, the optimal switching frequency depends on the input power and

voltage values, which, in PV applications, change continuously due to the intermittency of meteorological conditions. Thus, the proposed real-time tracking process must be executed when operating in the target PV field in order to optimally match the PV power converter operation to the PV generator characteristics and by that maximize the energy production of the overall PV system.

Compared to the conventional MPPT systems of prior art, two additional sensors are required for implementing the proposed technique, in order to measure the dc/dc converter output voltage and current, respectively. This increases the manufacturing cost of the proposed PV structures, which, however, is compensated by the higher energy production during the entire lifetime period of the PV system (e.g., 20–30 years), which is offered by applying the proposed technique, as demonstrated by the experimental results presented in this paper. Additionally, in case of battery-charging applications, both of these sensors must also be deployed for controlling the battery charging process, whereas if the dc/dc converter is connected to a grid-connected dc/ac inverter, then the output voltage sensor must also be used for controlling the dc/ac stage of the PV system [44].

## IV. CONCLUSION

The residential PV systems are highly prone to partial shading caused by nearby objects, which results in the power-voltage characteristic of the PV source to exhibit one or more local MPPs. The power production of the overall PV system can be maximized by applying a global MPPT method for ensuring that the PV array operates at the global MPP, where its power production is maximized, and, simultaneously, by dynamically maximizing the efficiency of the power converter that interfaces the PV-generated energy to the energy storage devices or the electric grid.

In this paper, a new control method has been presented for the real-time maximization of the output power production of PV systems. In the proposed technique, the duty cycle and switching frequency of the power converter PWM control signal are used as two independent control variables which are modified in real-time such that both the output power of the PV array and the output power of the power converter are maximized. Compared to the corresponding techniques presented till present in prior art, the proposed method can be applied in PV systems operating under partial-shading conditions. Also, knowledge of either the operational characteristics and configuration of the PV modules within the PV array or the power converter operational characteristics, is not required for its application. These features facilitate the use of the proposed technique in commercially available PV power converter products.

The experimental results validated that, by using the proposed method, the power production of the PV system is increased significantly compared to the case that only the power production of the PV array is maximized by using a global MPPT technique without tracking the optimal value of the power converter switching frequency. The proposed method has been applied in a boost-type dc/dc power converter for proof-of-concept purposes, but it can be easily extended for application in other types of dc/dc or dc/ac PV power converters.

The proposed technique can be adapted for application in combination with the PV array reconfiguration method presented in [45], which targets to maximize the service lifetime duration of the PV source, thus achieving the long-term maximization of the energy production of the overall PV system. Also, it can be incorporated in DMPPT systems for enhancing the PV system energy production in case of non-uniform incidence of solar irradiation at the individual solar cells synthesizing each PV module.

Current research work also includes the experimental application of alternative evolutionary optimization algorithms [2]–[10] instead of the PSO technique employed in this paper, for tracking the optimal values of the power converter duty cycle and switching frequency, in order to investigate comparatively their computation requirements, as well as their performance in terms of convergence speed and MPPT efficiency.

## REFERENCES

[1] "Global market outlook for solar power/2017-21," SolarPower Eur., Bruxelles, Belgium, Tech. Rep., 2017.

[2] S. Mohanty, B. Subudhi, and P. K. Ray, "A new MPPT design using Grey Wolf optimization technique for photovoltaic system under partial shading conditions," *IEEE Trans. Sustain. Energy*, vol. 7, no. 1, pp. 181–188, Jan. 2016.

[3] D. F. Teshome, C. H. Lee, Y. W. Lin, and K. L. Lian, "A modified firefly algorithm for photovoltaic maximum power point tracking control under partial shading," *IEEE J. Emerg. Sel. Topics Power Electron.*, vol. 5, no. 2, pp. 661–671, Jun. 2017.

[4] R. B. A. Koad, A. F. Zobaa, and A. El-Shahat, "A novel MPPT algorithm based on particle swarm optimization for photovoltaic systems," *IEEE Trans. Sustain. Energy*, vol. 8, no. 2, pp. 468–476, Apr. 2017.

[5] J. P. Ram, and N. Rajasekar, "A novel flower pollination based global maximum power point method for solar maximum power point tracking," *IEEE Trans. Power Electron.*, vol. 32, no. 11, pp. 8486–8499, Nov. 2017.

[6] N. Kumar, I. Hussain, B. Singh, and B. K. Panigrahi, "Single sensor-based MPPT of partially shaded PV system for battery charging by using Cauchy and Gaussian sine cosine optimization," *IEEE Trans. Energy Convers.*, vol. 32, no. 3, pp. 983–992, Sep. 2017.

[7] C. Huang, L. Wang, R. S.-C. Yeung, Z. Zhang, H. S.-H. Chung, and A. Bensoussan, "A prediction model-guided Jaya algorithm for the PV system maximum power point tracking," *IEEE Trans. Sustain. Energy*, vol. 9, no. 1, pp. 45–55, Jan. 2018.

[8] N. Kumar, I. Hussain, B. Singh, and B. K. Panigrahi, "Rapid MPPT for uniformly and partial shaded PV system by using JayaDE algorithm in highly fluctuating atmospheric conditions," *IEEE Trans. Ind. Inform.*, vol. 13, no. 5, pp. 2406–2416, Oct. 2017.

[9] K. S. Tey, S. Mekhilef, M. Seyedmahmoudian, B. Horan, A. T. Oo, and A. Stojcevski, "Improved differential evolution-based MPPT algorithm using SEPIC for PV systems under partial shading conditions and load variation," *IEEE Trans. Ind. Inform.*, vol. 14, no. 10, pp. 4322–4333, Oct. 2018.

[10] C. Manickam, G. P. Raman, G. R. Raman, S. I. Ganesan, and N. Chilakapati, "Fireworks enriched P&O algorithm for GMPPT and detection of partial shading in PV systems," *IEEE Trans. Power Electron.*, vol. 32, no. 6, pp. 4432–4443, Jun. 2017.

[11] J. Ahmed, and Z. Salam, "An improved method to predict the position of maximum power point during partial shading for PV arrays," *IEEE Trans. Ind. Inf.*, vol. 11, no. 6, pp. 1378–1387, Dec. 2015.

[12] A. Ramyar, H. Iman-Eini, and S. Farhangi, "Global maximum power point tracking method for photovoltaic arrays under partial shading conditions," *IEEE Trans. Ind. Electron.*, vol. 64, no. 4, pp. 2855–2864, Apr. 2017.

[13] X. Li, H. Wen, Y. Hu, L. Jiang, and W. Xiao, "Modified beta algorithm for GMPPT and partial shading detection in photovoltaic systems," *IEEE Trans. Power Electron.*, vol. 33, no. 3, pp. 2172–2186, Mar. 2018.

[14] Y. Mahmoud and E. F. El-Saadany, "A novel MPPT technique based on an image of PV modules," *IEEE Trans. Energy Convers.*, vol. 32, no. 1, pp. 213–221, Mar. 2017.

[15] H. M. El-Helw, A. Magdy, and M. I. Marei, "A hybrid maximum power point tracking technique for partially shaded photovoltaic arrays," *IEEE Access*, vol. 5, pp. 11900–11908, 2017.

[16] Y.-Tae Jeon and J.-Hu Park, "Unit-minimum least power point tracking for the optimization of photovoltaic differential power processing systems," *IEEE Trans. Power Electron.*, vol. 34, no. 1, pp. 311–324, Jan. 2019.

[17] A. Tomar, and S. Mishra, "Synthesis of a new DLMPPT technique with PLC for enhanced PV energy extraction under varying irradiance and load changing conditions," *IEEE J. Photovolt.*, vol. 7, no. 3, pp. 839–848, May 2017.

[18] S. Sajadian, and R. Ahmadi, "Distributed maximum power point tracking using model predictive control for photovoltaic energy harvesting architectures based on cascaded power optimizers," *IEEE J. Photovolt.*, vol. 7, no. 3, pp. 849–857, May 2017.

[19] M. Balato, L. Costanzo, and M. Vitelli, "Series-Parallel PV array reconfiguration: maximization of the extraction of energy and much more," *Appl. Energy*, vol. 159, pp. 145–160, 2015.

[20] Y. Hu, J. Zhang, P. Li, D. Yu, and L. Jiang, "Non-Uniform aged modules reconfiguration for large-scale PV array," *IEEE Trans. Device Mater. Rel.*, vol. 17, no. 3, pp. 560–569, Sep. 2017.

[21] Y. Mahmoud and E. F. El-Saadany, "Enhanced reconfiguration method for reducing mismatch losses in PV systems," *IEEE J. Photovolt.*, vol. 7, no. 6, pp. 1746–1754, Nov. 2017.

[22] Y. Kim, N. Chang, Y. Wang, and M. Pedram, "Maximum power transfer tracking for a photovoltaic-supercapacitor energy system," in *Proc. ACM/IEEE Int. Symp. Low-Power Electron. Des.*, 2010, pp. 307–312.

[23] M. Adly and K. Strunz, "Irradiance-Adaptive PV module integrated converter for high efficiency and power quality in standalone and DC microgrid applications," *IEEE Trans. Ind. Electron.*, vol. 65, no. 1, pp. 436–446, Jan. 2018.

[24] Z. Chen, H. Wu, K. Sun, L. Ni, and Y. Xing, "Light-Load efficiency optimization for module integrated converters in photovoltaic systems," in *Proc. IEEE Energy Convers. Congr. Expo.*, 2013, pp. 5560–5565.

[25] Z. Zhang, M. Chen, M. Gao, Q. Mo, and Z. Qian, "An optimal control method for grid-connected photovoltaic micro-inverter to improve the efficiency at light-load condition," in *Proc. IEEE Energy Convers. Congr. Expo.*, 2011, pp. 219–224.

[26] Z. Zhang, M. Gao, Q. Mo, M. Chen, and Z. Qian, "Loss-Model based interleave technique to improve the efficiency of micro-inverter," in *Proc. 37th Annu. Conf. IEEE Ind. Electron. Soc.*, 2011, pp. 3888–3893.

[27] F. Reverter and M. Gasulla, "Optimal inductor current in boost DC/DC converters regulating the input voltage applied to low-power photovoltaic modules," *IEEE Trans. Power Electron.*, vol. 32, no. 8, pp. 6188–6196, Aug. 2017.

[28] M. Pahlevaninezhad, S. Pan, and P. Jain, "Dynamic maximum efficiency tracker for PV micro-inverter," U.S. Patent Appl. U.S. 2017/0117822 A1, Apr. 2017.

[29] D.-H. Kim and B.-K. Lee, "An enhanced control algorithm for improving the light-load efficiency of noninverting synchronous Buck–Boost converters," *IEEE Trans. Power Electron.*, vol. 31, no. 5, pp. 3395–3399, May 2016.

[30] H.-D. Gui, Y. Zhang, Z. Zhang, and Y.-F. Liu, "An optimized efficiency-based control strategy for islanded paralleled PV micro-converters," in *Proc. IEEE Appl. Power Electron. Conf. Expo.*, 2015, pp. 229–234.

[31] C.-S. Kwon, W.-K. Choi, and F.-S. Kang, "Maximum efficiency point tracking algorithm for photovoltaic power generating system," in *Proc. 2nd Pac.-Asia Conf. Circuits, Commun. Syst.*, 2010, vol. 1, pp. 71–74.

[32] K. Hyung, H. Shin, J.-I. Ha, and A. Yoo, "Efficiency control of multistring PV system considering switching losses analysis," in *Proc. IEEE Appl. Power Electron. Conf. Expo.*, 2014, pp. 3143–3149.

[33] F. Bez, L. Scandola, L. Corradini, S. Saggini, and G. Spiazzi, "Two-dimensional online efficiency optimization technique for dual active bridge converters," in *Proc. IEEE 17th Workshop Control Model. Power Electron.*, 2016, pp. 1–8.

[34] S. H. Kang, D. Maksimović, and I. Cohen, "Efficiency optimization in digitally controlled flyback DC-DC converters over wide ranges of operating conditions," *IEEE Trans. Power Electron.*, vol. 27, no. 8, pp. 3734–3748, Aug. 2012.

[35] J. A. Abu-qahouq, H. Mao, H. J. Al-atrash, and I. Batarseh, "Maximum efficiency point tracking (MEPT) method and digital dead time control implementation," *IEEE Trans. Power Electron.*, vol. 21, no. 5, pp. 1273–1281, Sep. 2006.

[36] M. M. Jovanović, and B. T. Irving, "On-the-fly topology-morphing control-efficiency optimization method for LLC resonant converters operating in wide input- and/or output-voltage range," *IEEE Trans. Power Electron.*, vol. 31, no. 3, pp. 2596–2608, Mar. 2016.

[37] N. Mohan, T. M. Undeland, and W. P. Robbins, "*Power Electronics: Converters, Applications, and Design*, 3rd ed. New York, NY, USA: Wiley, 2002.

[38] N. Femia, G. Petrone, G. Spagnuolo, and M. Vitelli, "A technique for improving P&O MPPT performances of double-stage grid-connected photovoltaic systems," *IEEE Trans. Ind. Electron.*, vol. 56, no. 11, pp. 4473–4482, Nov. 2009.

[39] M. Balato, L. Costanzo, P. Marino, G. Rubino, L. Rubino, and M. Vitelli, "Modified TEODI MPPT technique: Theoretical analysis and experimental validation in uniform and mismatching conditions," *IEEE J. Photovolt.*, vol. 7, no. 2, pp. 604–613, Mar. 2017.

[40] S. B. Kjaer, J. K. Pedersen, and F. Blaabjerg, "A review of single-phase grid-connected inverters for photovoltaic modules," *IEEE Trans. Ind. Appl.*, vol. 41, no. 5, pp. 1292–1306, Sep./Oct. 2005.

[41] Q. Li, and P. Wolfs, "A review of the single phase photovoltaic module integrated converter topologies with three different DC link configurations," *IEEE Trans. Power Electron.*, vol. 23, no. 3, pp. 1320–1333, May 2008.

[42] I. Seedadan and R. Wongsathan, "Fuzzy controller based maximum power point tracking technique of standalone photovoltaic module for lead-acid battery charging," in *Proc. 3rd Int. Conf. Control, Automat. Robot.*, 2017, pp. 598–601.

[43] R. Errouissi, S. M. Muyeen, A. Al-Durra, and S. Leng, "Experimental validation of a robust continuous nonlinear model predictive control based grid-interlinked photovoltaic inverter," *IEEE Trans. Ind. Electron.*, vol. 63, no. 7, pp. 4495–4505, Jul. 2016.

[44] F. Blaabjerg, and D. M. Ionel Eds., *Renewable Energy Devices and Systems With Simulations in MATLAB and ANSYS*, 1st ed. Boca Raton, FL, USA: CRC Press, 2017.

[45] M. Balato, L. Costanzo, and M. Vitelli, "Reconfiguration of PV modules: A tool to get the best compromise between maximization of the extracted power and minimization of localized heating phenomena," *Solar Energy*, vol. 138, pp. 105–118, 2016.

**Eftichios Koutroulis** (M'10–SM'15) was born in Chania, Greece, in 1973. He received the B.Sc. and M.Sc. degrees in electronic and computer engineering, in 1996 and 1999, respectively, and the Ph.D. degree in the areas of power electronics and renewable energy sources from the School of Electronic and Computer Engineering, Technical University of Crete, Chania, Greece, in 2002.

He is currently an Associate Professor with the School of Electrical and Computer Engineering, Technical University of Crete, where he also serves as the Director of the Circuits, Sensors and Renewable Energy Sources Laboratory. His research interests include power electronics, the development of microelectronic energy management systems for RES, and the design of photovoltaic and wind energy conversion systems.

**Nektarios Sason** was born in Athens, Greece, in 1991. He received the B.Sc. degree from the School of Electrical and Computer Engineering, Technical University of Crete, Chania, Greece, in 2018.

His current research interests are in the areas of power electronic converters for photovoltaic power production systems.

**Vasileios Georgiadis** was born in Athens, Greece, in 1994. He received the B.Sc. degree from the School of Electrical and Computer Engineering, Technical University of Crete, Chania, Greece, in 2018.

His research interests are currently focused on the development of control systems for photovoltaic power electronic converters.